

Scaling of submonolayer island sizes in surfactant-mediated epitaxy of semiconductors

Vasily Cherepanov, Sergey Filimonov, Josef Mysliveček, and Bert Voigtländer*

*Institut für Schichten und Grenzflächen (ISG 3) and cni-Center of Nanoelectronic Systems for Information Technology,
Forschungszentrum Jülich, 52425 Jülich, Germany*

(Received 16 March 2004; published 5 August 2004)

We study submonolayer island size distributions in the epitaxy of Si and Ge on the Si(111) surface with Bi as a surfactant. We show that sizes of Si islands at different growth temperatures scale to a standard scaling function that peaks at the mean island size. Size distribution of Ge islands demonstrates qualitatively different behavior: With the decreasing temperature the most probable size in the population of Ge islands shifts towards small island sizes so that the peaked scaling function degenerates to a decreasing one. The observed scaling phenomena are found to be inherent to the mechanism of growth which involves exchange and de-exchange processes of deposited atoms with the surfactant and the strong passivation of step edges in the presence of the surfactant.

DOI: 10.1103/PhysRevB.70.085401

PACS number(s): 68.55.Ac, 68.47.Fg, 81.15.Hi, 81.15.Aa

INTRODUCTION

Experimental investigations of density and size distribution of submonolayer island populations yield qualitative and in certain cases even quantitative information regarding microscopic mechanisms that determine the growth of the system under scrutiny. One particular type of information is whether the studied growth system classifies within a standard growth model or not. In the standard growth model,¹ atoms arrive at a substrate with a flux F and diffuse on the substrate with a temperature dependent diffusion rate D . No desorption of atoms from the surface is allowed. When two or more diffusing atoms meet a two-dimensional (2D), one monolayer (ML) high island nucleates and grows further by the diffusion limited capture of adatoms. In this way a population of 2D islands covering a fraction θ of the surface develops. In the precoalescence regime of growth the island population is characterized by the island size distribution N_s . For various amounts of deposited material expressed in terms of the surface coverage θ , N_s scales onto a single function $f(x)$:

$$N_s = \theta \langle s \rangle^{-2} f(s/\langle s \rangle), \quad (1)$$

where $\langle s \rangle$ denotes the mean island size.² In the standard growth model $f(x)$ is a peak function with a peak at $x=1$.²⁻⁵ In addition, the total island density N is a power law of F and D :¹

$$N \propto (F/D)^\chi, \quad 1/3 \leq \chi < 1. \quad (2)$$

When the above conditions are met, predictions of the standard growth model can be used to measure D and other model parameters.^{6,7}

On the other hand, the experimentally observed deviations from the behavior predicted by Eqs. (1) and (2) can be used to identify important growth mechanisms beyond the standard model. Examples include observations of growth with $\chi=0$ in systems with post-deposition⁸ or displacive^{9,10} nucleation, occurrence of a decreasing scaling function $f(x)$ caused by these mechanisms⁸⁻¹⁰ or by a strong anisotropy of the surface structure,¹¹ growth with $\chi>1$ in systems with hindered incorporation of atoms into the islands,^{12,13} and the

observation of a multipeak island size distribution when stable islands of “magic” sizes exist.¹⁴ Additionally, transition from a peaked scaling function to a decreasing one with the increasing growth temperature was predicted theoretically for systems with prominent desorption of deposited particles.^{15,16}

In surfactant mediated epitaxy (SME)¹⁷⁻²¹ particles of the deposited material arrive at a surface, where a monolayer of another species, so called surfactant, is adsorbed. This modifies the growth scenario compared to the growth without surfactant, allowing, e.g., layer-by-layer growth of relaxed layers in highly strained Ge/Si heteroepitaxy.^{18,19} Therefore SME systems are good candidates to have a behavior different from that predicted by the standard growth model. Indeed, $\chi>1$ was measured in submonolayer growth of Ge on the Pb-covered Si(111) surface.²² Meanwhile, no measurements of the island size distributions in SME have been reported so far.

In this work, we present the first experimental study of submonolayer island size distributions in SME. We use a scanning tunneling microscope (STM) to observe the morphology of Si and Ge layers grown on Si(111) by SME with Bi as a surfactant (Bi-SME). We find scaling of N_s according to Eq. (1) for both Si and Ge. For Si, a standard scaling function is observed. For Ge, a scaling function with a peak strongly shifted towards small island sizes is found. This nonstandard scaling is temperature dependent: for higher temperatures, the scaling function approaches the standard one. We demonstrate, that the observed scaling phenomena can be explained considering exchange and deexchange processes of deposited atoms with surfactant and the passivation of step edges in the presence of surfactant.²³ For this purpose, we perform kinetic Monte Carlo (KMC) simulations of a generalized diffusion–de-exchange–passivation (DDP) model of surfactant mediated epitaxy.²⁴ In terms of the DDP model, stronger passivation of the step edges for Ge atoms than for Si atoms is required to obtain the experimentally observed difference of the submonolayer scaling in Ge and Si Bi-MBE on the Si(111) surface.

EXPERIMENT

Experiments were performed in an ultrahigh vacuum chamber with a base pressure $<5 \times 10^{-11}$ Torr. Si(111) substrates doped to $1 \times 10^{19} \text{ cm}^{-3}$ Sb were resistively heated by passing dc current. Standard flashing procedure yielded clean Si(111) 7×7 surface. This surface was kept at 500°C and terminated by Bi evaporated at a rate 1 BL/min (1 BL = 1.56×10^{15} atoms/cm²) from a Knudsen cell. After Bi termination, substrate temperature was set to a desired level and Ge or Si was deposited from a graphite or tantalum crucible, respectively, both heated by electron bombardment. Bi was codeposited at a rate 1 BL/min and the characteristic Bi-induced $\sqrt{3} \times \sqrt{3}$ surface structure was maintained during growth.

Scaling of N_s was studied for layers grown at $F=0.2$ BL/min and θ from 0.06 BL to 0.2 BL. Substrate temperatures were set to 440°C for Ge layers and 480°C for Si layers to obtain a comparable island density in both systems. Typical surface morphology of a Ge and a Si layer is shown in Figs. 1(a) and 1(b). Surface morphology of the Ge layer distinctly differs from that of the Si layer: islands of different sizes, among them many small islands are observed in the Ge layer, whereas in the Si layer the island sizes are more uniform.

This observation is further supported by a comparison of the island size distributions N_s for Ge and Si that are shown in Figs. 1(c) and 1(d), respectively.²⁵ In both cases, we observe a fit of the rescaled N_s for different θ onto a single scaling function. The scaling function peaks at $s=\langle s \rangle$ for Si, however, the peak is found at $s < 0.2\langle s \rangle$ for Ge. Thus, Ge SME on Bi-terminated Si(111) is not described by the standard nucleation model. For both Ge and Si, additional measurements were performed at complementary temperatures 480°C for Ge and 440°C for Si. These reveal, that N_s for Ge approaches a normal one with increasing temperature [Fig. 1(c)]. N_s for Si does not change [Fig. 1(d)].

It is well established that the island size distribution is rather sensitive to the spatial correlations of the island locations.²⁶ A measure of the spatial arrangement of islands in the experiment is the nearest-neighbor separation distribution $N(r)$.²⁷ This quantity represents the density of islands having its nearest neighbor at a distance r . It scales as $N(r) = Ng(r/\langle r \rangle)$ where $\langle r \rangle$ denotes a mean distance to a nearest neighbor. Rescaled $N(r)$ for Ge and Si are shown in Figs. 1(e) and 1(f). In contrast to the Si case the rescaled $N(r)$ is asymmetric for Ge with the peak shifted toward smaller island sizes. This is an indication of a certain loss of spatial correlation²⁷ between Ge islands compared to Si islands. The islands can nucleate at smaller relative separations in the Ge layer than in the Si layer. A similar effect can be observed at preexisting step edges on the Si(111) substrate, as seen in Fig. 2. Islands can nucleate very close to the step edge in the Ge layer [Fig. 2(a)]. On the contrary, in the Si layer a pronounced denuded zone²⁸ free of islands appears [Fig. 2(b)].

To complete the experimental picture of Ge and Si Bi-SME on the Si(111) surface, we measured the exponent χ of Eq. (2). The value of χ for Ge and Si was determined from values of N obtained at five different settings of F . F was

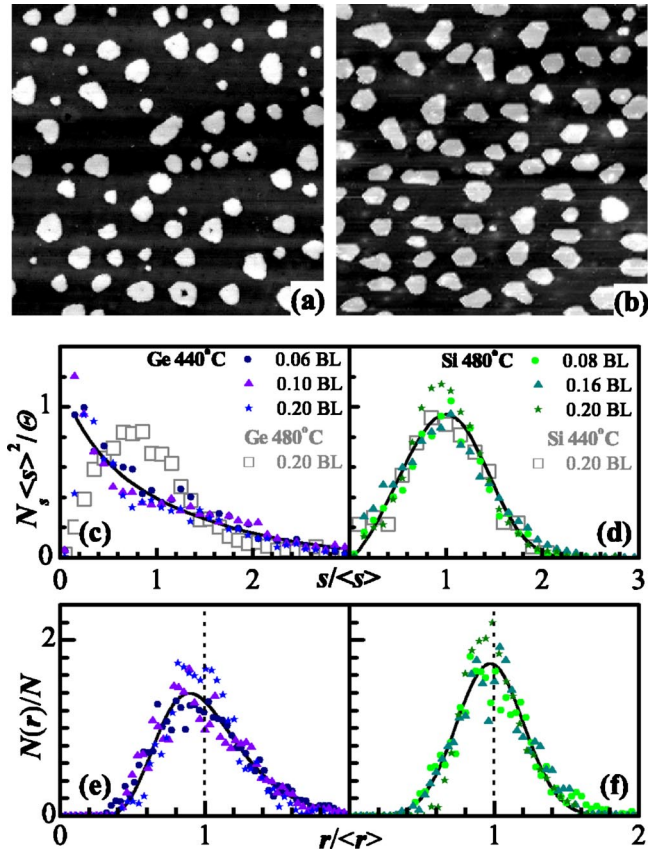


FIG. 1. (Color online) Morphology of (a) Ge layer, (b) Si layer grown by Bi-SME on the Si(111) surface. $\theta=0.2$ BL, $F=0.2$ BL/min. $T=440^\circ\text{C}$ for Ge, $T=480^\circ\text{C}$ for Si. Image width is 210 nm in (a), 140 nm in (b). (c), (d) Corresponding plots of the rescaled N_s for various θ (closed symbols), measurement of N_s for complementary temperatures (open symbols). (e), (f) Corresponding rescaled nearest neighbor separation distribution $N(r)$ of islands in Ge and Si layer. Lines represent guides to the eye (Ref. 42).

varied between 0.08 BL/min and 6.3 BL/min, θ was set to 0.2 BL and T to 440°C for both Ge and Si. We obtain similar values $\chi_{\text{Ge}}^{440^\circ\text{C}}=0.37 \pm 0.02$ for Ge and $\chi_{\text{Si}}^{440^\circ\text{C}}=0.36 \pm 0.02$ for Si, within standard limits for χ .

The observed nonstandard scaling in Bi-SME of Ge on Si(111) differs from all observations of nonstandard sub-

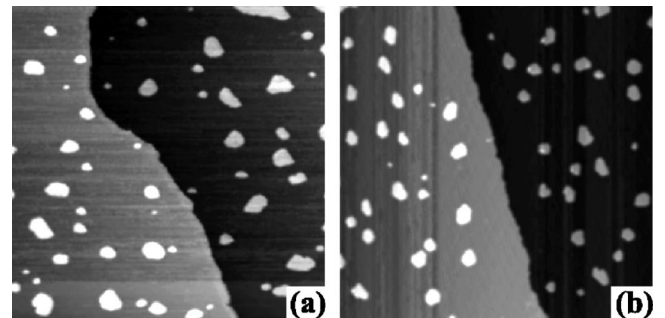


FIG. 2. Island population near a step edge in (a) Ge layer, (b) Si layer grown by Bi-SME on the Si(111) surface. $\theta=0.1$ BL, $F=0.2$ BL/min, $T=440^\circ\text{C}$ for Ge, $\theta=0.08$ BL, $F=0.2$ BL/min, $T=480^\circ\text{C}$ for Si. Image width is 230 nm in (a), 130 nm in (b).

monolayer scaling mentioned above. The observed scaling function for N_s is not multipeak.¹⁴ Rather, it can be approximated by a decreasing function [Fig. 1(c)]. Such a behavior cannot be related to post-deposition⁸ or displacive^{9,10} nucleation, because a nonzero exponent $\chi_{\text{Ge}}^{440^\circ\text{C}}$ is observed. Arguments on pronounced anisotropy¹¹ do not apply to the $\sqrt{3} \times \sqrt{3}$ structure of the Bi-terminated Si(111) surface. A transition between the peaked and decaying scaling functions due to desorption^{15,16} can be excluded as the expected temperature dependence for this desorption-induced phenomenon is opposite to that observed in our study.

We will not consider eventual strain contributions to the scaling phenomena observed in our experiments. The strain contributions to submonolayer island scaling have so far been detected only in semiconductor heteroepitaxy on surfaces with pronounced anisotropy, in particular, by evaluating the distribution of projections of island sizes onto two nonequivalent directions.^{29,30} In addition, the observed difference between the rescaled N_s of a strained system [Ge on Bi-terminated Si(111)] and an unstrained system [Si on Bi-terminated Si(111)] is much larger than the effects of strain on the scaling of N_s predicted for isotropic systems.^{31,32}

DIFFUSION-DE-EXCHANGE-PASSIVATION MODEL OF SME

The deviation of the scaling observed in Bi-mediated growth of Ge on Si(111) from the predictions of the standard growth model justifies a search for additional atomic-scale processes which could contribute to the observed scaling phenomena. In the following, we will study the scaling of N_s in the diffusion-de-exchange-passivation model of SME proposed in Refs. 23 and 24.

The DDP model assumes three basic processes that happen during the SME growth (Fig. 3): diffusion of deposited atoms on top of the surfactant, exchange of material atoms with surfactant to incorporate below the surfactant layer, and de-exchange of material atoms with surfactant atoms to get back on top of the surfactant. Processes are considered to be thermally activated with rates ν_i having an Arrhenius form $\nu_i = \nu_0 \exp(-E_i/k_B T)$, where ν_0 is the common prefactor of the order 10^{13} s^{-1} , k_B is the Boltzmann's constant, T temperature, and E_i the activation energy of the i th process with E_D , E_{ex} , E_{dex} standing for diffusion, exchange and de-exchange processes, respectively. Generally, $E_{\text{dex}} > E_{\text{ex}}$, to account for the increase of the binding energy of single material atoms upon incorporation. Important is a definition of the behavior of material atoms at step edges. In the DDP model, not only terraces but also step edges are passivated, i.e., incorporation of atoms into step edges does not happen automatically. Upon incorporation of an atom at the step edge, its binding energy increases more than that of an atom on the terrace. Accordingly, E_{dex} at step edges is larger than E_{dex} for staying alone atoms.

The above described DDP model was used to show, that the island density N in SME depends on a combination of E_D , E_{ex} , E_{dex} ,²⁴ rather than on E_D only as is in the standard model.¹ Thus, observations of N in SME are not directly related to the E_D as was expected in earlier works.^{20,21} It has

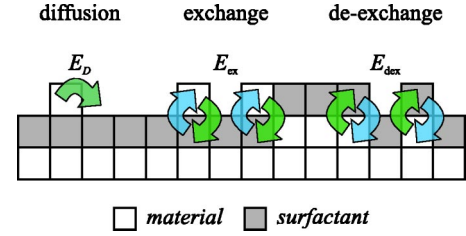


FIG. 3. (Color online) Growth processes considered in the DDP model of SME (Refs. 23 and 24). Related activation energies of these processes E_D , E_{ex} , E_{dex} generally differ for material atoms in plane and material atoms at step edges.

also been demonstrated,²³ that assuming a proper strain dependence of E_{dex} at step edges, the experimentally observed transition from 2D growth at low temperatures to 3D growth at high temperatures²⁰ can be explained.

To study scaling of submonolayer island size distributions we generalized the DDP model in terms of the well established bond-counting KMC scheme of epitaxial growth,^{3,4} which is well suited for such purposes. In this scheme, the activation energy of a growth process for a particular atom depends on a number n of its nearest lateral neighbors. Thus, in the DDP model, the activation energy for diffusion of atoms on top of the surfactant becomes $E_D = E_s + n_{\text{top}} E_n^{\text{top}}$, where E_s is the activation energy for hopping of a single atom on top of the surfactant, and $n_{\text{top}} E_n^{\text{top}}$ is the increase of the binding energy of an atom before a hop due to n_{top} nearest lateral neighbors. Additional energy barriers to hopping of atoms across the step edges³³ are not considered. For simplicity, no difference between surfactant and material neighbors on top of the surfactant is made. The activation energy for exchange E_{ex} is kept constant independent of n_{top} , which ensures the passivation of the step edges in the DDP model.^{23,24}

Due to incorporation below surfactant, atoms increase their binding energy by $E_{\text{inc}} + n_{\text{inc}} E_n^{\text{inc}}$ with respect to single atoms on top of the surfactant. The linear term $n_{\text{inc}} E_n^{\text{inc}}$ represents the step edge contribution to the binding energy, n_{inc} is the number of nearest neighbors of an atom that are incorporated below surfactant. The de-exchange happens with an activation energy $E_{\text{dex}} = E_{\text{ex}} + E_{\text{inc}} + n_{\text{inc}} E_n^{\text{inc}} - n_{\text{top}} E_n^{\text{top}}$ which accounts properly for the difference of binding energies of an atom that is determined by n_{inc} before and n_{top} after de-exchange.

We employed an unrestricted solid-on-solid simulation scheme on a square lattice with a periodic boundary condition.^{3,4} Simulation events have been selected with a standard algorithm.³⁴ To save the computation time we set F and T to values that yield island sizes approximately 20 times smaller compared to those in the experiment. The parameters E_s , E_{ex} , and E_{inc} determining the behavior of single atoms in the DDP model have been selected in accord with *ab initio* calculations of the activation energies for hopping, exchange, and de-exchange of single Si and Ge atoms on the As-terminated Si(111) surface.³⁵

The major qualitative predictions of Ref. 35 can be summarized as follows. First, the activation energies E_s for hopping are equal in both systems (0.25 eV). Second, the acti-

vation energy E_{ex} for exchange of a single Si atom (0.27 eV) is close to the hopping barrier E_s , i.e., Si atoms easily incorporate under the surfactant layer. In contrast, Ge atoms have to overcome a significantly higher exchange barrier (0.71 eV) and therefore they can stay longer on top of the surfactant. Third, the activation energies for de-exchange $E_{\text{dex}}=E_{\text{ex}}+E_{\text{inc}}$ are, in fact, comparable for both materials (1.07 eV for Si and 0.9 eV for Ge). Assuming a similar qualitative behavior on the Bi-terminated Si(111) surface³⁶ we used two different sets of parameters in our KMC simulations of Si and Ge deposition: $E_s=0.3$ eV, $E_{\text{ex}}=0.3$ eV, $E_{\text{inc}}=0.3$ eV for Si, and $E_s=0.3$ eV, $E_{\text{ex}}=0.5$ eV, $E_{\text{inc}}=0.1$ eV for Ge. The binding energies E_n^{top} and E_n^{inc} , as well as the attempt frequency ν_0 were set to be equal for both materials with $E_n^{\text{inc}}=0.25$ eV, $E_n^{\text{top}}=0.05$ eV,³⁷ and $\nu_0=2 \times 10^{12}$ s⁻¹. To clearly identify one of the possible reasons for the experimentally observed difference in scaling of N_s in Ge and Si Bi-SME on Si(111), the activation energies in our KMC simulation differ only in the activation energy of exchange E_{ex} for Ge and Si parameters.

It should be emphasized that in our study we concentrated on the *qualitative* scaling behavior and did not intend to reproduce *quantitative* features. Therefore, the parameters listed above cannot be regarded as a fit of the DDP model to the experimental data. Still, a considerable agreement with the experiment is achieved.

In Figs. 4 and 5 results of the KMC simulation of the DDP model are presented. Simulations were performed at $F=0.2$ BL/s, $T=320$ K for Ge parameters, and $T=400$ K for Si parameters. At these temperatures, the model yields the island density that differs by less than 10% for both materials. As in the experiment, to obtain similar densities of Ge and Si islands, a lower temperature in Ge growth than in Si growth must be used.

Figures 4(a) and 4(b) show the morphologies obtained from the simulations with the two sets of parameters. In agreement with experiment, a more regular pattern of islands is observed with Si parameters.

Figures 4(c) and 4(d) show the rescaled island size distribution N_s obtained from simulations with Ge and Si parameters at different θ . Scaling of N_s with θ , characterized by a decreasing scaling function for Ge parameters at 320 K and a normal peaked scaling function for Si parameters at 400 K is obtained in agreement with experiment. Simulations at complementary temperatures of 380 K for Ge and 340 K for Si reveal that a normal scaling behavior with a peaked size distribution of Ge islands is recovered with the increasing T . For Si parameters, no significant change of N_s within the temperature interval comparable to the experimental one is observed.

Figures 4(e) and 4(f) show the rescaled nearest-neighbor separation distribution $N(r)$ obtained from simulations with Ge and Si parameters. In agreement with the experiment, the rescaled $N(r)$ for Ge parameters is biased towards small island separations, while for Si parameters, the rescaled $N(s)$ is symmetric. This indicates nucleation of islands at smaller relative separations in the simulation with Ge parameters than with Si parameters. The appearance of the denuded zones has also been reproduced correctly in the

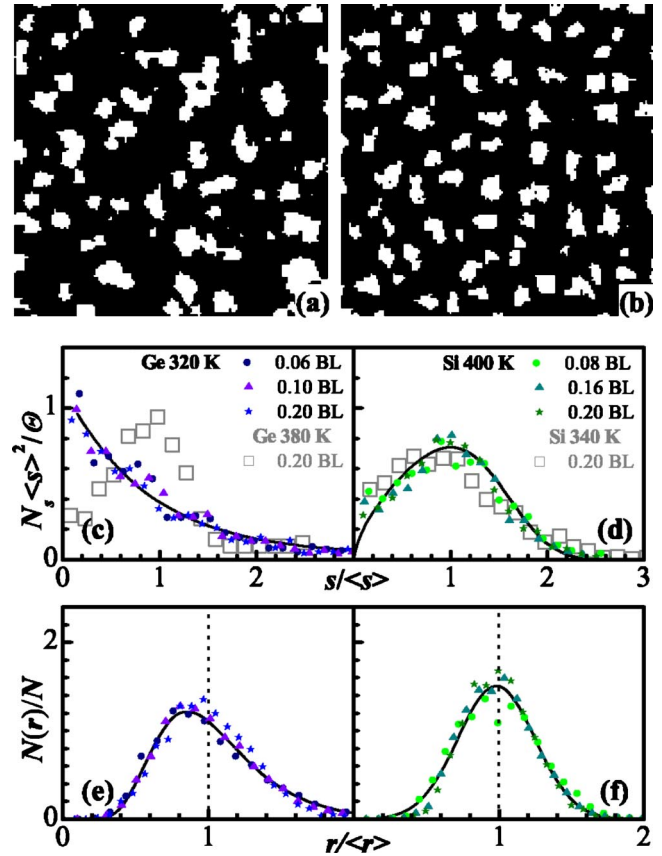


FIG. 4. (Color online) Morphology obtained from KMC simulations of the DDP model of SME. (a) Ge parameters, (b) Si parameters. $\theta=0.2$ BL, $F=0.2$ BL/s. $T=320$ K for Ge, $T=400$ K for Si. Image width is 150 lattice units (of 512). (c), (d) Corresponding plots of the rescaled N_s from simulation at various θ (closed symbols), simulation of N_s for complementary temperatures (open symbols). (e), (f) Corresponding rescaled nearest neighbor separation distribution $N(r)$ of islands obtained from simulation for Ge and Si parameters. Lines represent guides to the eye (Ref. 42).

simulation (Fig. 5), showing no denuded zone for Ge parameters [Fig. 5(a)], and a pronounced denuded zone for Si parameters [Fig. 5(b)].

Finally, values of χ have been measured in the simulation for Ge parameters at 320 K and Si parameters at 340 K. χ

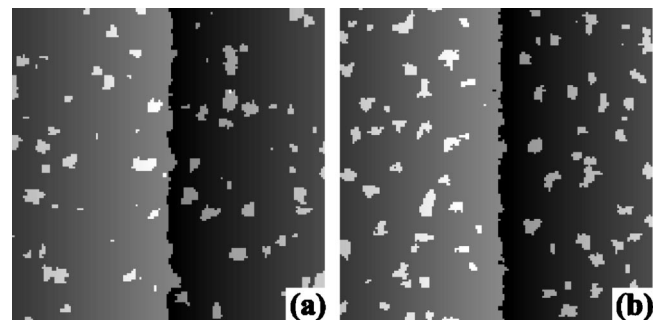


FIG. 5. Island population near a step edge as obtained from KMC simulations of the DDP model of SME. (a) Ge parameters, (b) Si parameters. $\theta=0.1$ BL, $F=0.2$ BL/s. $T=320$ K for Ge, $T=440$ K for Si. Image width is 150 lattice units (of 256).

was determined from a dependence of N on F for 5 values of F between 0.1 BL/s and 2 BL/s. We obtain $\chi_{\text{Ge}}^{320\text{ K}} = 0.41 \pm 0.02$ in good agreement with experiment. $\chi_{\text{Si}}^{340\text{ K}} = 0.28 \pm 0.02$ underestimates the related experimental value, however, is still near the lower limit predicted theoretically for χ in the standard growth model [Eq. (2)].³⁸

DISCUSSION

Results of our KMC simulations of SME allow to formulate new implications of the DDP model. Particularly, under certain conditions, the DDP model yields a nonstandard decreasing scaling function for the distribution N_s of submonolayer island sizes. This nonstandard scaling behavior is temperature dependent: at higher temperatures, the island size distribution N_s obeys the normal scaling with a peak at $s = \langle s \rangle$. The appearance of the decaying scaling function in the DDP model is accompanied by the narrowing of denuded zones around step edges and islands.

In order to understand the origin of the nonstandard scaling behavior we recall that it was observed in our simulations using the Ge parameter set only, while with the Si parameters the standard peaked scaling function was reproduced at all considered temperatures. The main difference of the two sets of parameters is the value of the activation energy E_{ex} needed for incorporation of the deposited atoms below the surfactant layer via the exchange process. In comparison with the barrier to diffusion of deposited atoms on top of the surfactant $E_{\text{ex}}(\text{Ge}) > E_{\text{hop}}(\text{Ge})$ for Ge, while $E_{\text{ex}}(\text{Si}) = E_{\text{hop}}(\text{Si})$ for Si. This means that almost every hop of a Si atom on top of the surfactant is followed by an exchange/de-exchange event. Therefore, Si atoms reaching the step edge position will exchange and attach to the Si step edge with a high probability. On the contrary, Ge atoms on top of the surfactant make many hops before an exchange/de-exchange event (≈ 5000 hops before an exchange event for single atoms and Ge parameters at 320 K). This causes that Ge atoms reaching the step edge position can leave this position with much higher probability than to exchange and attach to the step edge. In other words, in the DDP model the step edges with the Ge parameter set are passivated much stronger than with the Si parameter set. Therefore, the nonstandard scaling phenomena in the DDP model can be regarded as a result of the strong passivation of step edges in the presence of surfactant.

The main consequence of the strong step edge passivation is the transition from growth limited by the surface diffusion to growth limited by the attachment kinetics.³⁹ In the latter case the adatom distribution between step edges becomes uniform.³⁹ Therefore the nucleation of new islands occurs with equal probability across the surface and no correlation in the island locations is observed. In this situation the nucleation kinetics resembles in many respects the nucleation ki-

netics in the Kolmogorov-Avrami model,^{40,41} which, indeed, predicts a decreasing power-law scaling function for island sizes.²⁷ The asymmetric shape of the nearest-neighbor separation distribution $N(r)$ as observed in our experiments for Ge islands was also proposed to be a signature of the growth mode with the uniform adatom density.²⁷

Another signature of the growth mediated by the incorporation kinetics could be a flux dependence of the total island density with the exponent $\chi > 1$.¹³ However, both for Si and Ge our study revealed $\chi < 0.5$, i.e. lower than the lower limit predicted for this case by the theory.¹³ This shows that the island size distribution is more sensitive to the actual regime of growth than the total island density.

As the deposition temperature increases the role of the exchange barrier vanishes and the kinetic regime of the island growth can change to the diffusion one.³⁹ In accord, the standard peaked island size distribution recovers, as observed in our experiments and reproduced by KMC simulations. A similar temperature transition from a decreasing scaling function for N_s to a standard one was predicted for epitaxy with desorption of atoms from the surface.^{15,16} However, the decreasing scaling function occurs at high temperatures in this case. This is caused by the fact that the desorption influences the adatom density that becomes constant at high temperatures.¹⁶

CONCLUSIONS

In this work, we present the first experimental study of submonolayer island size distributions in surfactant mediated epitaxy (SME). We find scaling of island sizes to a standard scaling function in Bi-mediated SME of Si on Si(111). On the contrary, distribution of island sizes in Bi-mediated SME of Ge on Si(111) scales to a nonstandard scaling function with a peak that is strongly shifted towards small island sizes. This nonstandard scaling in Ge SME is temperature dependent. For higher temperatures, the scaling function approaches the standard one.

Using kinetic Monte Carlo simulations, we demonstrate, that the observed scaling phenomena can be explained considering exchange and de-exchange processes of Ge and Si atoms with the surfactant layer and a passivation of step edges on the Si(111) surface due to the presence of surfactant.^{23,24} The different scaling phenomena in Bi-mediated SME of Ge and Si on Si(111) can be explained considering a stronger passivation of step edges for the Ge atoms on the Bi-terminated Si(111) surface than for Si atoms.

ACKNOWLEDGMENTS

We would like to thank Neelima Paul for fruitful discussions and Helmut Stollwerk and Peter Coenen for the technical assistance. The stay of S.F. and J.M. in Germany was supported by the Alexander von Humboldt Foundation.

*Electronic address: b.voigtlaender@fz-juelich.de

- ¹A. Pimpinelli and J. Villain, *Physics of Crystal Growth* (Cambridge University Press, Cambridge, 1998).
- ²M.C. Bartelt and J.W. Evans, *Phys. Rev. B* **46**, 12675 (1992).
- ³C. Ratsch, A. Zangwill, P. Šmilauer, and D.D. Vvedensky, *Phys. Rev. Lett.* **72**, 3194 (1994).
- ⁴C. Ratsch, P. Šmilauer, A. Zangwill, and D.D. Vvedensky, *Surf. Sci.* **329**, L599 (1995).
- ⁵J. Amar and F. Family, *Phys. Rev. Lett.* **74**, 2066 (1995).
- ⁶J.A. Strosio and D.T. Pierce, *Phys. Rev. B* **49**, R8522 (1994).
- ⁷H. Brune, G.S. Bales, J. Jacobsen, C. Boragno, and K. Kern, *Phys. Rev. B* **60**, 5991 (1999).
- ⁸B. Müller, L. Nedelmann, B. Fischer, H. Brune, and K. Kern, *Phys. Rev. B* **54**, 17858 (1996).
- ⁹D.D. Chambliss and K.E. Johnson, *Phys. Rev. B* **50**, 5012 (1994).
- ¹⁰A. Zangwill and E. Kaxiras, *Surf. Sci.* **326**, L483 (1995).
- ¹¹B.A. Joyce, D.D. Vvedensky, A.R. Avery, J.G. Belk, H.T. Dobbs, and T.S. Jones, *Appl. Surf. Sci.* **98**, 357 (1998).
- ¹²L. Andersohn, Th. Berke, U. Köhler, and B. Voigtländer, *J. Vac. Sci. Technol. A* **14**, 312 (1996).
- ¹³D. Kandel, *Phys. Rev. Lett.* **78**, 499 (1997).
- ¹⁴B. Voigtländer, M. Kästner, and P. Šmilauer, *Phys. Rev. Lett.* **81**, 858 (1998).
- ¹⁵P. Jensen, H. Larralde, and A. Pimpinelli, *Phys. Rev. B* **55**, 2556 (1997).
- ¹⁶P.A. Mulheran and D.A. Robbie, *Philos. Mag. B* **80**, 1299 (2000).
- ¹⁷M. Copel, M.C. Reuter, E. Kaxiras, and R.M. Tromp, *Phys. Rev. Lett.* **63**, 632 (1989).
- ¹⁸M. Horn-von Hoegen, F.K. LeGoues, M. Copel, M.C. Reuter, and R.M. Tromp, *Phys. Rev. Lett.* **67**, 1130 (1991).
- ¹⁹G. Meyer, B. Voigtländer, and N.A. Amer, *Surf. Sci.* **274**, L541 (1992).
- ²⁰B. Voigtländer and A. Zinner, *J. Vac. Sci. Technol. A* **12**, 1932 (1994).
- ²¹B. Voigtländer, A. Zinner, T. Weber, and H.P. Bonzel, *Phys. Rev. B* **51**, 7583 (1995).
- ²²I.-S. Hwang, T.-C. Chang, and T.T. Tsong, *Phys. Rev. Lett.* **80**, 4229 (1998).
- ²³D. Kandel and E. Kaxiras, *Phys. Rev. Lett.* **75**, 2742 (1995).
- ²⁴D. Kandel and E. Kaxiras, *Solid State Phys.* **54**, 219 (2000).
- ²⁵For the evaluation of N_s , areas on the surface not influenced by step edges, domain boundaries and Si islands created during Bi termination were selected.
- ²⁶C. Ratsch, M.F. Gyure, S. Chen, M. Kang, and D.D. Vvedensky, *Phys. Rev. B* **61**, R10598 (2000).
- ²⁷P.A. Mulheran and D.A. Robbie, *Philos. Mag. Lett.* **78**, 247 (1998).
- ²⁸J.A. Venables, *Surf. Sci.* **299**, 798 (1994).
- ²⁹V. Bressler-Hill, S. Varma, A. Lorke, B.Z. Nosho, P.M. Petroff, and W.H. Weinberg, *Phys. Rev. Lett.* **74**, 3209 (1995).
- ³⁰B.Z. Nosho, V. Bressler-Hill, S. Varma, and W.H. Weinberg, *Surf. Sci.* **364**, 164 (1996).
- ³¹C. Ratsch, A. Zangwill, and P. Šmilauer, *Surf. Sci.* **314**, L937 (1994).
- ³²S. Tan and P.-M. Lam, *Phys. Rev. B* **59**, 5871 (1999).
- ³³P. Šmilauer, M.R. Wilby, and D.D. Vvedensky, *Phys. Rev. B* **47**, 4119 (1993).
- ³⁴A.B. Bortz, M.H. Kalos, and J.L. Lebowitz, *J. Comput. Phys.* **17**, 10 (1975).
- ³⁵K. Schroeder, A. Antons, R. Berger, and S. Blügel, *Phys. Rev. Lett.* **88**, 046101 (2002).
- ³⁶K. Schroeder (private communication); K. Schroeder, A. Antons, R. Berger, and S. Blügel, *Phase Transitions* **75**, 91 (2002).
- ³⁷ $E_n^{\text{inc}} > E_n^{\text{top}}$ ensures that virtually all deposited atoms incorporate below surfactant during growth.
- ³⁸An increase of simulated $\chi_{\text{Si}}^{340\text{ K}}$ can be obtained by lowering E_n^{inc} in Si parameters, however, on the costs of readjusting other Si parameters to obtain an agreement with other experimental data. The concern of this work is to keep Si and Ge parameter sets as similar as possible.
- ³⁹I. Markov, *Surf. Sci.* **429**, 102 (1999).
- ⁴⁰A.N. Kolmogorov, *Bull. Acad. Sci. USSR, Phys. Ser. (Engl. Transl.)* **1**, 335 (1937).
- ⁴¹M. Avrami, *J. Chem. Phys.* **7**, 1103 (1939).
- ⁴²The lines are (c) a double exponential, (d) an analytical expression for rescaled N_s proposed in Ref. 5, (e) a log-normal distribution, and (f) a normal distribution.